Historical Change and Future Scenarios of Sea Level Rise in Macau and Adjacent Waters

Lin WANG[1], Gang HUANG[*,2,3], Wen ZHOU[4], and Wen CHEN[5]

[1]*Key Laboratory of Regional Climate–Environment for Temperature East Asia, Institute of Atmospheric Physics, Chinese Academy of Sciences, Beijing 100029*

[2]*State Key Laboratory of Numerical Modeling for Atmospheric Sciences and Geophysical Fluid Dynamics, Institute of Atmospheric Physics, Chinese Academy of Sciences, Beijing 100029*

[3]*Joint Center for Global Change Studies, Beijing 100875*

[4]*Guy Carpenter Asia–Pacific Climate Impact Centre, School of Energy and Environment, City University of Hong Kong, Hong Kong*

[5]*Center for Monsoon System Research, Institute of Atmospheric Physics, Chinese Academy of Sciences, Beijing 100190*

ABSTRACT

Against a background of climate change, Macau is very exposed to sea level rise (SLR) because of its low elevation, small size, and ongoing land reclamation. Therefore, we evaluate sea level changes in Macau, both historical and, especially, possible future scenarios, aiming to provide knowledge and a framework to help accommodate and protect against future SLR. Sea level in Macau is now rising at an accelerated rate: 1.35 mm yr^{-1} over 1925–2010 and jumping to 4.2 mm yr^{-1} over 1970–2010, which outpaces the rise in global mean sea level. In addition, vertical land movement in Macau contributes little to local sea level change. In the future, the rate of SLR in Macau will be about 20% higher than the global average, as a consequence of a greater local warming tendency and strengthened northward winds. Specifically, the sea level is projected to rise 8–12, 22–51 and 35–118 cm by 2020, 2060 and 2100, respectively, depending on the emissions scenario and climate sensitivity. Under the $+8.5$ W m^{-2} Representative Concentration Pathway (RCP8.5) scenario the increase in sea level by 2100 will reach 65–118 cm—double that under RCP2.6. Moreover, the SLR will accelerate under RCP6.0 and RCP8.5, while remaining at a moderate and steady rate under RCP4.5 and RCP2.6. The key source of uncertainty stems from the emissions scenario and climate sensitivity, among which the discrepancies in SLR are small during the first half of the 21st century but begin to diverge thereafter.

Key words: Macau, sea level rise, emissions scenario, climate sensitivity, vertical land movement, uncertainty

---

1. Introduction

Macau (22°10'N, 113°33'E), a special administrative region of China, is located on the southern coast of China, on the South China Sea (Fig. 1). Its territory consists of Macau Peninsula and the islands of Taipa and Coloane, totaling 30.3 km² up to 2014. In fact, the total area of Macau was only 2.78 km² in the 17th century, but it has been enlarged by 50% since 1912 because of land reclamation efforts. Currently, land reclamation in Macau is still ongoing. In addition, Macau has generally flat terrain, with the lowest point being 0 m. Due to its low-lying elevation and significant coastal development, Macau faces huge risks from sea level rise (SLR).

As reported by Church and White (2006) and Nerem et al. (2010), global mean sea level (GMSL) has been rising at a rate of 1.7 ± 0.3 mm yr^{-1} over the last century, while during the last 20 years it has risen to 3.3 ± 0.4 mm yr^{-1}, suggesting that SLR is accelerating. SLR due to global warming is a serious global threat, especially for Macau, where a large population, economic activity, and important cultural features are situated. Generally, SLR has a far-reaching and pronounced impact on coastal assets through increased coastal erosion, higher surge flooding, landward intrusion of seawater, and more extensive coastal inundation. As indicated by Nicholls and Cazenave (2010), the future of China's coastline appears to be highly threatened by SLR.

To reduce the risk of current and future SLR, great effort has been expended in studying it at both global and local scales. Here, we focus on sea level change at the local level, which has particular relevance for local policymaking. Several research teams have conducted assessments of sea

---

* Corresponding author: Gang HUANG
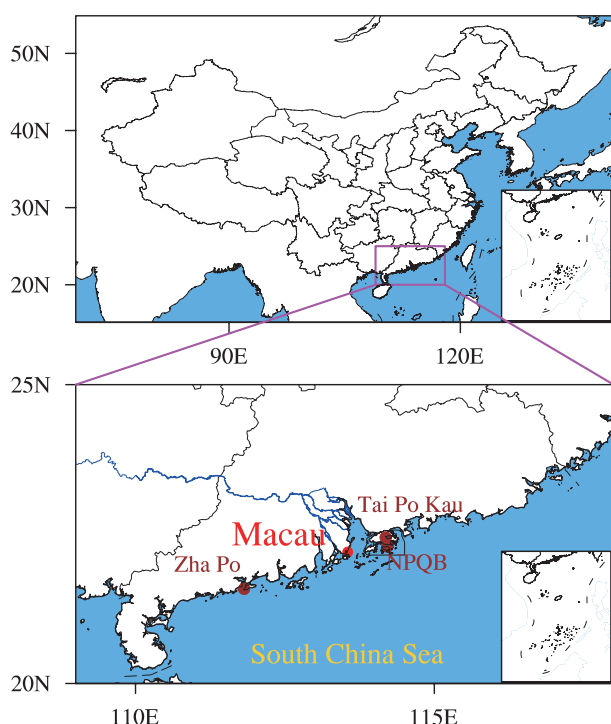
  Email: hg@mail.iap.ac.cn

Fig. 1. Geographical location of Macau (red dot) along with Zha Po, Tai Po Kau and North Point Quarry Bay (NPQB) (brown dots) in China.

level change associated with a given city: for example, Chen and Omstedt (2005) discussed the climate-induced sea level variation in Stockholm from 1873 to 1995; Moron and Ullmann (2005) investigated the relationship between sea level pressure and sea level height in Camargue; and Stephens and Bell (2009) reviewed the coastal inundation and SLR in Nelson, New Zealand. Regarding coastal cities in China, Ding et al. (2001), BakiIz and Shum (2000), Li and Mok (2011) and Wong et al. (2003) all examined the long-term sea level change in Hong Kong, the other special administrative region of China; and He et al. (2014) estimated regional sea level change in the Pearl River Delta. Despite significant sea level research, there are no studies dealing specifically with sea level change in Macau. Moreover, few studies have emphasized future changes in sea level, which is crucial to advance planning for adaptive strategies.

Generally, the rise of sea level not only has tremendous impact on Macau, but affects any coastal lowland. Nevertheless, compared to other port cities along the coastal margins of China, Macau is most susceptible to SLR-induced hazards. On the one hand, because of limited land areas, the landward migration of coastal assets and communities will be much more constrained. On the other hand, Macau has the largest land reclamation programs in China, which in turn exacerbates the threats from SLR. Hence, Macau is most concerned about the potential SLR in future brought by climate change and mitigation strategies to deal with associated detrimental consequences. In light of the high priority for addressing sea level-related issues in Macau, we carry out a comprehen-

sive evaluation of historical and possible future changes in Macau. Meanwhile, although concentrating on the Macau region, this study is expanded to encompass the neighboring corridor along the coasts of southern China (SC).

This paper is structured as follows: The tide gauge, satellite and model-based data are described in section 2. Section 3 presents the detail of the methodology used for constructing a relative sea level (RSL) scenario. The historical change of sea level in Macau and adjacent waters is demonstrated in section 4, followed by projected future scenarios in section 5. Finally, section 6 summarizes the key conclusions with some discussion of related issues.

2. Data

2.1. *Tide gauge measurements*

Hourly tidal data in Macau for the period 1925–2010, gathered by the Macau Meteorological and Geophysical Bureau, are used in this study. To remove short-term fluctuation, such as diurnal and semidiurnal oscillations, the monthly mean sea levels are computed from hourly tidal records. Note that tide gauges measure the sea level relative to a fixed benchmark on nearby land, so tide gauge observations consist of signals from both sea level change and vertical land motion. Therefore, tide gauges measure RSL change.

To detect how global change influences local sea level in Macau, the GMSL dataset of the same time span is retrieved from the Commonwealth Scientific and Industrial Research Organisation, available at http://www.cmar.csiro.au/sealevel/sl_data_cmar.html. The reconstruction product is developed by Church and White (2011) based on *in-situ* sea level data from coastal tide gauges worldwide.

Historical tide gauge observations other than Macau along the SC coast are obtained from the Permanent Service for Mean Sea Level (PSMSL) databank (http://www.psmsl.org/). Established in 1933, the PSMSL has been responsible for the collection, publication, analysis and interpretation of sea level data from the global network of tide gauges. The time series of tidal measurements produced by the PSMSL have been adjusted to a common datum, called Revised Local Reference, which is defined to be approximately 7000 mm below the mean sea level. Only stations with sufficient records that span at least 30 years are considered for this study. The names, geographic distribution and data length of the three selected stations are shown in Table 1 and Fig. 1.

2.2. *Satellite altimetry data*

Gridded satellite data of sea level anomalies are obtained from AVISO (Archiving, Validation and Interpretation of Satellite Oceanographic Data) (Dibarboure et al., 2014), which is a merged product based on altimetry data from Topex/Poseidon, Jason-1, ERS-1 and ERS-2, and EnviSat. The near-global sea level anomaly data are available on a $0.25° \times 0.25°$ latitude–longitude grid from 1993 to 2012 at monthly intervals. In addition, the AVISO data are provided in the form of anomalies compared to the 20-yr mean from

1993 to 2012. Relevant information about the altimetry data and detailed procedures used in the generation of AVISO can be found at http://www.aviso.altimetry.fr. In contrast to tide gauge observations, satellite altimetry measurements are carried out in a geocentric reference frame; in other words, relative to the center of the Earth. Therefore, satellite altimetry measures absolute sea level (ASL) change.

2.3. CMIP5 multi-model outputs

To assess potential future changes in sea level, data from 24 coupled climate models are downloaded from the Coupled Model Intercomparison Project Phase 5 (CMIP5) (Tay-

lor et al., 2012). Table 2 summarizes information about the models used in this study and their associated organizations. Thanks to SimCLIM software, the sea level data have been processed with a pattern scaling technique and subsequently downscaled to a common $0.5° \times 0.5°$ latitude–longitude grid. Therefore, we employ the refined data provided by the Sim-CLIM software rather than the raw model output. To encompass a broad range of scenarios in expected sea level change, a full suite of emissions levels, including the $+2.6$ W m^{-2} Representative Concentration Pathway(RCP2.6) scenario, RCP4.5, RCP6.0, and RCP8.5 (Moss et al., 2010), is used. Besides model-based sea level data, forcing scenar-

Table 1. Tide gauge stations along the SC coast used for this study, along with their latitude–longitude locations and recording periods.

Station name	Location	Recording period	Data source
Macau	(22.2°N, 113.55°E)	1925–2010	Macau Meteorological and Geophysical Bureau
Zha Po	(21.583°N, 111.817°E)	1959–2014	PSMSL
Tai Po Kau	(22.443°N, 114.184°E)	1963–2013	PSMSL
North Point Quarry Bay	(22.291°N, 114.213°E)	1950–2013	PSMSL

Table 2. Summary of the 24 climate models from CMIP5 used in this study.

Model	Modeling center
bcc-csm1-1	Beijing Climate Center, China Meteorological Administration
bcc-csm1-1-m	Beijing Climate Center, China Meteorological Administration
CanESM2	Canadian Centre for Climate Modelling and Analysis
CCSM4	National Center for Atmospheric Research
CMCC-CMS	Centro Euro-Mediterraneo per I Cambiamenti Climatici
CMCC-CM	Centro Euro-Mediterraneo per I Cambiamenti Climatici
CNRM-CM5	Centre National de Recherches Météorologiques/Centre Européen de Recherche et Formation Avancée en Calcul Scientifique
CSIRO-Mk3-6-0	Commonwealth Scientific and Industrial Research Organization in collaboration with Queensland Climate Change Centre of Excellence
GFDL-CM3	NOAA Geophysical Fluid Dynamics Laboratory
GFDL-ESM2G	NOAA Geophysical Fluid Dynamics Laboratory
GFDL-ESM2M	NOAA Geophysical Fluid Dynamics Laboratory
GISS-E2-R-CC	NASA Goddard Institute for Space Studies
GISS-E2-R	NASA Goddard Institute for Space Studies
HadGEM2-CC	Met Office Hadley Centre (additional HadGEM2-ES realizations contributed by Instituto Nacional de Pesquisas Espaciais)
HadGEM2-ES	Met Office Hadley Centre (additional HadGEM2-ES realizations contributed by Instituto Nacional de Pesquisas Espaciais)
inmcm4	Institute for Numerical Mathematics
MIROC5	Atmosphere and Ocean Research Institute (The University of Tokyo), National Institute for Environmental Studies, and Japan Agency for Marine-Earth Science and Technology
MIROC-ESM	Japan Agency for Marine-Earth Science and Technology, Atmosphere and Ocean Research Institute (The University of Tokyo), and National Institute for Environmental Studies
MIROC-ESM-CHEM	Japan Agency for Marine-Earth Science and Technology, Atmosphere and Ocean Research Institute (The University of Tokyo), and National Institute for Environmental Studies
MPI-ESM-LR	Max-Planck-Institut für Meteorologie (Max Planck Institute for Meteorology)
MPI-ESM-MR	Max-Planck-Institut für Meteorologie (Max Planck Institute for Meteorology)
MRI-CGCM3	Meteorological Research Institute
NorESM1-M	Norwegian Climate Centre
NorESM1-ME	Norwegian Climate Centre

ios of relevant variables including ocean heat content (OHC) for total column, and meridional wind under RCP4.5 and RCP8.5, are also investigated, in order to gain better insight into sea level issues. OHC in this study is defined as the vertical average of ocean potential temperature from the surface to the sea floor, according to the equation

$$\mathrm{OHC} = \frac{1}{z} \int_0^z \theta(z)dz \,, \tag{1}$$

in which θ is the potential temperature and 0 and z represent sea surface and sea floor depth. Note that the definition of OHC here differs from the classical one, but they have essentially the same physical sense. In addition, following the latest progress by the Intergovernmental Panel on Climate Change (IPCC), the 30-yr period from 1986 to 2005 is chosen for the baseline climate.

3.   Methodology

3.1.   *Components of RSL change*

It is relative rather than absolute SLR that requires planning in a given region. In general, RSL change for a specific site can be attributed to a combination of three main components (Nicholls et al., 2011):

(1) GMSL rise. This reflects the change in the global volume of the ocean, which is primarily due to thermal expansion of the ocean as it warms and the melting of glaciers and ice sheets.

(2) Departures from the global average. This is caused by non-uniform distributions of temperature change, along with spatially varying responses of atmospheric and oceanic circulation to climate change. The regional departures can be as much as 50%–100% from the global average.

(3) Vertical land movement (VLM). In general, VLM occurs owing to various natural and anthropogenic geological processes. The former include tectonic activity, glacial isostatic adjustment, and earthquakes, while the latter involve groundwater extraction and drainage. The inclusion of VLM is critical to the determination of RSL change, since its magnitude could be appreciable in its effects on SLR itself. A landmass can rise, subside, or remain stable. The subsidence of land exacerbates the adverse impact of SLR, while uplift processes alleviate it. For example, the sea level at Stockholm is falling by a few millimeters per year because of land emergence in response to the disappearance of ice during the last deglaciation; in contrast, Manila has experienced considerable land settlement induced by intensive ground pumping, which enhances the local SLR.

Direct monitoring of VLM is accomplished through continuous GPS. Unfortunately, there is no such measurement at Macau. Nevertheless, an alternative and indirect approach is still available to recover the VLM. Because altimetry and tide gauges measure ASL and RSL, respectively, and ASL, RSL and VLM are interrelated by $\mathrm{RSL} = \mathrm{ASL} - \mathrm{VLM}$, on the one hand the sea level difference between altimetry and tide gauge data is dominated by VLM, while on the other

hand geological processes are so slow that they are usually considered linear on a time scale of a few centuries (Chen and Omstedt, 2005). Consequently, the linear trend of sea level difference (altimetry minus tide gauge) is the proxy of the local rate of VLM. This method has been extensively explored and validated in many works, e.g., Cazenave et al. (1999), García et al. (2007), and Ray et al. (2010).

In short, regional RSL rise can be readily derived by integrating the above three components of sea level change using the following expression:

$$\Delta\mathrm{RSL} = \Delta\mathrm{GMSL} + \Delta\mathrm{SL_R} - \Delta\mathrm{VLM} \,, \tag{2}$$

where $\Delta\mathrm{RSL}$ is the change in RSL for a given site, $\Delta\mathrm{GMSL}$ is the change in GMSL, $\Delta\mathrm{SL_R}$ is the regional deviation in sea level from the global average, and $\Delta\mathrm{VLM}$ is the change in local VLM.

3.2.   *SimCLIM software*

SimCLIM is an integrated software package designed for impact and adaptation assessment related to climate change and variability (Warrick et al., 2005). It is one of the tools recommended by the United Nations Framework Convention on Climate Change in the area of impact and vulnerability analyses. Currently, SimCLIM runs on the latest CMIP5 datasets and supports four RCP emission scenarios (RCP2.6, RCP4.5, RCP6.0, and RCP8.0). One of the major features of Sim-CLIM is a sea level scenario generator. For generating future projected sea level changes, SimCLIM adopts a "pattern scaling" method that involves the use of spatial output from complex coupled atmosphere–ocean circulation models in conjunction with projections of global-mean climate changes deduced from a simple climate model. The pattern scaling method was initiated by Santer et al. (1990) and has received widespread use in the construction of climate scenarios (Walsh et al., 1998; Mitchell, 2003). This technique is based on the theory that a simple climate model is capable of representing a global climate response, even when the response is nonlinear and a wide range of climatic variables are a linear function of the amount of global warming. To derive the scaling pattern, the spatial sea level change, produced by a coupled climate model, is divided by the corresponding global mean obtained from a simple climate model. The ratio, also called the scaling factor, in each grid is interpreted as the local change with respect to the per unit change in the global mean. Therefore, the scaling factor indicates whether the local SLR will be equal to (scaling factor = 1), greater than (>1), or less than (<1) the global average value. For example, if the local ratio is 1.25, then for every centimeter rise of GMSL, the local rise will be 1.25 cm.

4.   Historical sea level change and estimate of VLM

The monthly mean sea level at Macau relative to the local chart datum is given in Fig. 2. The chart datum in Macau is defined to be 1.8 m and 2.34 m below mean sea level for
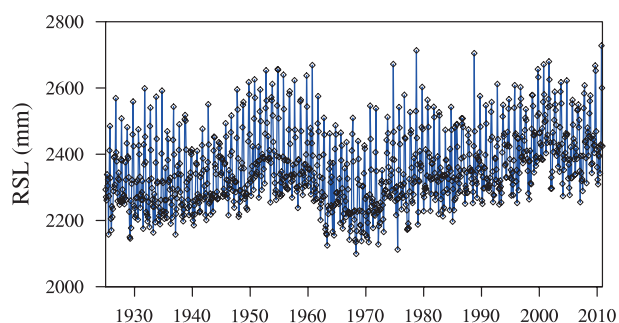
Fig. 2. Temporal evaluation of RSL at Macau (units: mm) in reference to local chart datum.

the periods 1925–1966 and 1967 to present, respectively. To remove the datum discontinuity, the monthly means have been reduced to a common datum: 2.34 m below mean sea level. An overall upward trend of RSL is revealed at a rate of 1.35 mm yr^{-1}. However, the rising trend is not monotonic but dominated by multidecadal variability. From the mid-1950s

to 1970s, the sea level generally falls, with a linear trend of -9.6 mm yr^{-1}. Since the 1970s, the sea level in Macau has risen significantly, at a rate of 4.2 mm yr^{-1}.

Figure 3 illuminates the possible links between sea level changes in Macau and GMSL. Although seemingly close to linear, the evolution of GMSL does contain decadal-scale fluctuation, as illustrated in Fig. 3d. It is noticeable that the GMSL also experienced a similar regime shift from the 1950s to the early 1970s, but with weak amplitude. Further, the 27-yr sliding correlation shown in Fig. 3e confirms the temporal consistency between the detrended sea level in Macau and the GMSL before the mid-1970s, suggesting that global-scale change may have played a crucial role in shaping the sea level in Macau prior to the mid-1970s. However, such an association tends to break down after 1970, implying that sea level change due to local and regional factors dominates from the mid-1970s onward. These conjectures need to be proven through extensive diagnoses and experimentation, but it is beyond the scope of this study to go into such detail.

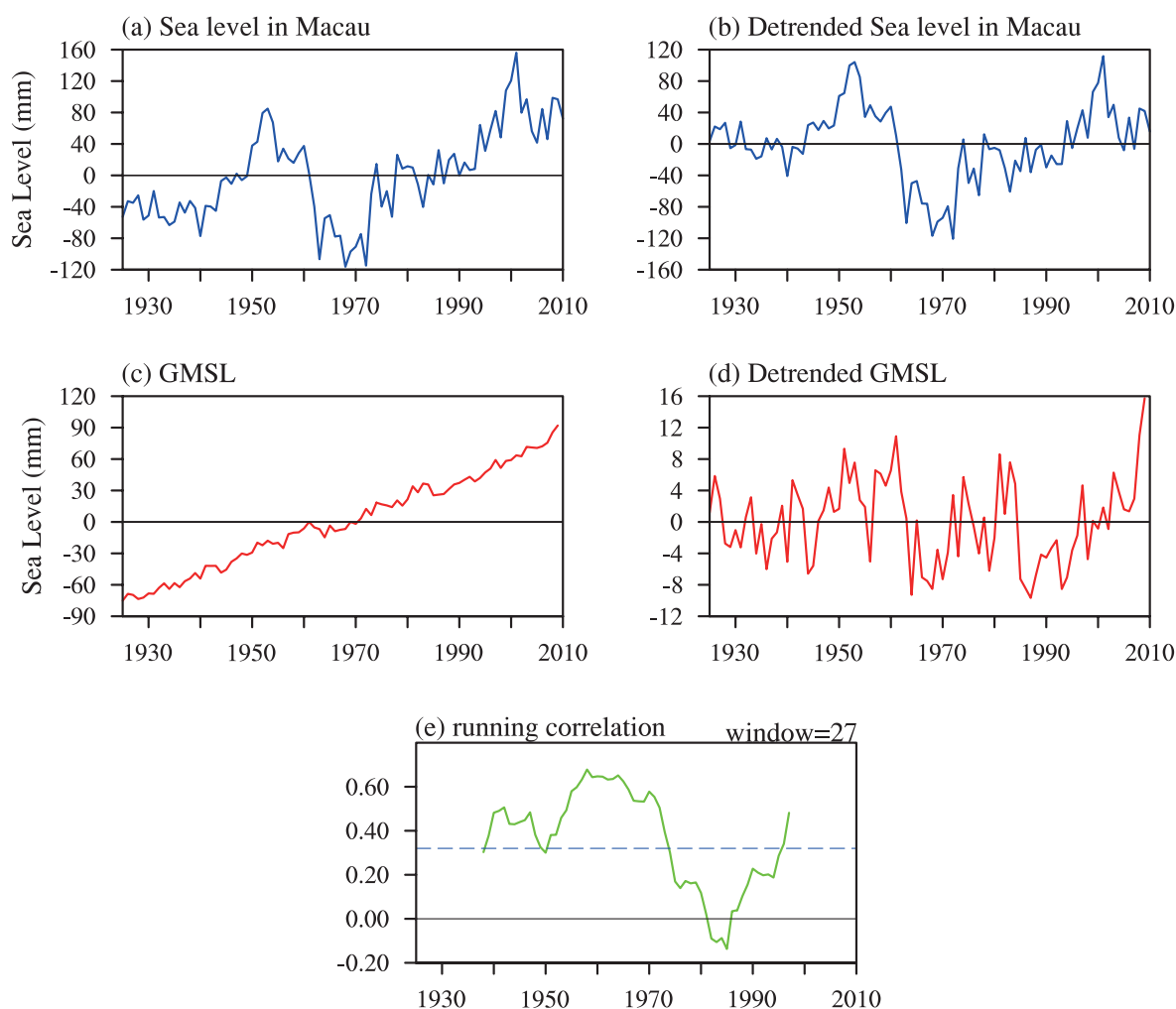The historical perspective of sea water levels adjacent to

Fig. 3. (a, b) Time Series of annual sea level anomalies in Macau relative to the entire period and those with secular trend removed; (c, d) same as a and b, but for global mean sea level (GMSL); (e) 27-year running correlation between detrended sea level in Macau and GMSL. Correlations are computed over 27-year segments moving from the beginning to the end of the records. The blue dashed line marks the critical correlation coefficient (0.32) at a confidence level of 90%.
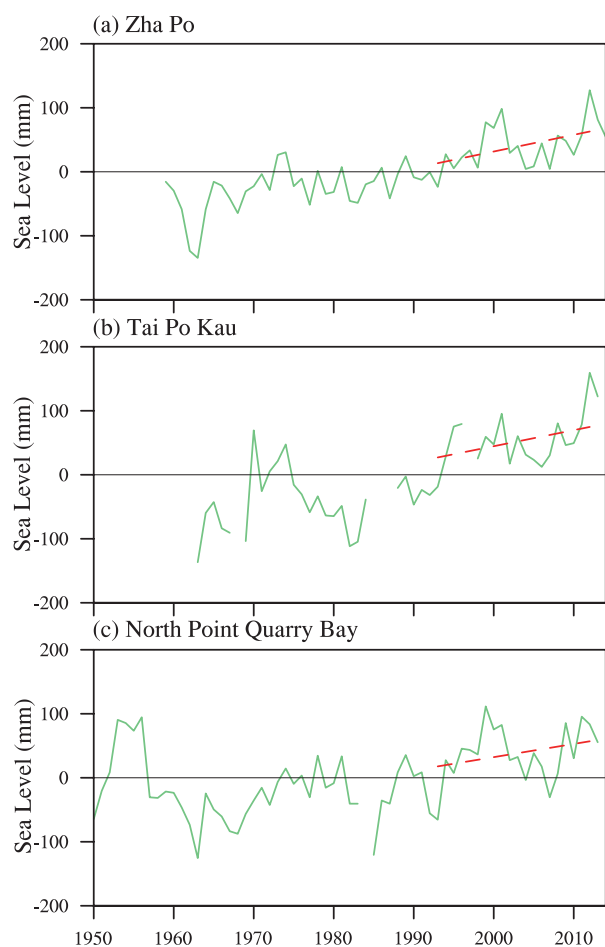
Fig. 4. Annual sea level anomalies at Zha Po (a), Tai Po Kau (b), North Point Quarry Bay (c) from 1950 to 2014. Red dashed line denotes the linear trend over the period of 1993 to 2012.

which have record lengths of more than 30 years. It is noticeable that the temporal pattern of sea level observed at Zha Po, Tai Po Kau and North Point Quarry Bay are remarkably similar to that over Macau, with a rapid decline from 1950 to around 1970 followed by a general upward trend since then. The sea levels at the three tide gauge sites are highly correlated with that for Macau, with correlation coefficients of 0.79, 0.69 and 0.73, respectively. Also, the sea level at these three tide gauges rose at a rate of 2.6, 2.5 and 2 mm yr^{-1} during the period 1993–2012, significant at the 95% confidence level. On the whole, the sea level oscillations in the historical perspective are found to exhibit regional-scale spatially coherent signals across the shoreline band of SC.

From the perspective of satellite altimetry, as shown in Fig. 5 [also reported by the IPCC's Fifth Assessment Report (AR5)], sea level has not risen uniformly worldwide during the satellite era (1993–2012). In some regions, such as the eastern Pacific, rates of sea level change are slower than the global average, or even negative. However, the western Pacific is characterized by pronounced greater-than-average SLR. This is also the case for Macau, whose rate of SLR since 1993 amounts to 3.2 mm yr^{-1}, higher than the global mean rate of about 2.9 mm yr^{-1}. Moreover, as we will see in section 5, the sea level at Macau will continue to rise faster than the global mean in the future.

Since VLM is essential to the local effects of SLR, the most important task is to estimate the VLM at Macau following the procedure outlined in section 3.1. The monthly sea level difference, altimetry minus tide gauge, is calculated over 1993–2010. Figure 6a displays the monthly altimetry and tide gauge sea level at Macau. These two time series are highly coherent, with a correlation coefficient of 0.83. The sequence of altimeter minus gauge differences is shown in Fig. 6b, with the linear fit imposed. As indicated by the linear trend, the rate of VLM at Macau is estimated at −0.153 mm yr^{-1}, accumulating only 1.53 cm of subsidence over a span of one century. An identical outcome can also be achieved if we rely on the annual average time series (figure not shown).
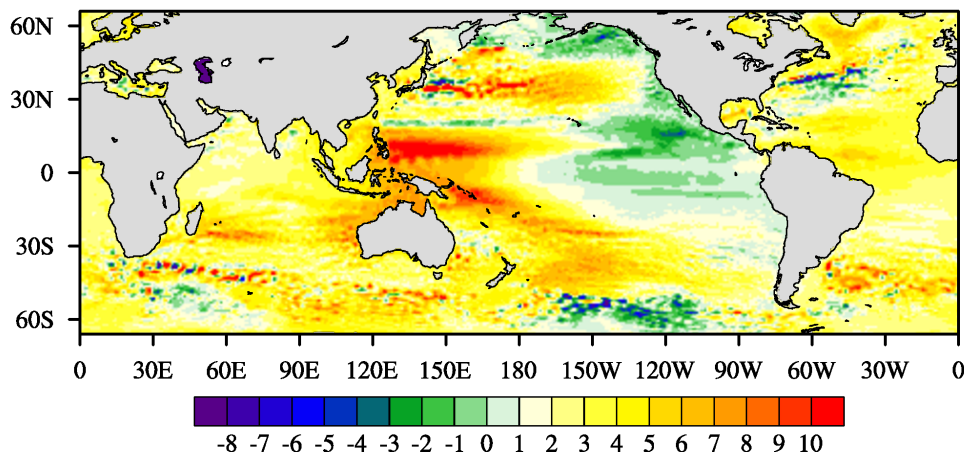
Macau is examined next. Figure 4 demonstrates the evolution of annual sea level with the long-term climatological mean removed at Zha Po, Tai Po Kau and North Point Quarry Bay,

Fig. 5. Spatial pattern in sea level trends (units: mm yr^{-1}) for the period 1993 to 2012 based on AVISO.
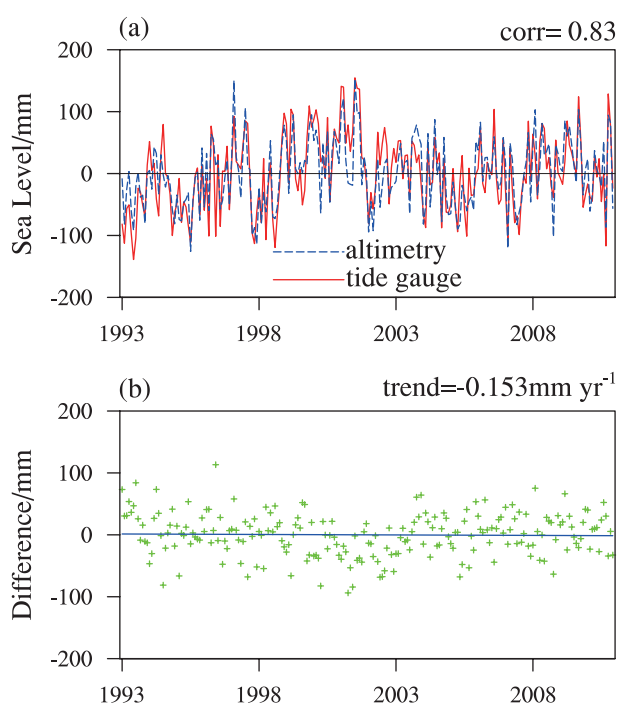
Fig. 6. (a) Altimetric (blue dashed line) and tide gauge (red solid line) sea level anomalies at Macau from 1993 to 2010 at monthly intervals, and (b) their difference (green dots) along with the fitted linear regression (blue line).

Consequently, it can be concluded that Macau has virtually no vertical motion. Finally, it is necessary to emphasize that the tendency of VLM is computed indirectly; if geodetic measures from GPS are launched in the future, VLM will be estimated more accurately.

5. Future scenarios of SLR

Prior to model projections of future sea level in Macau and adjacent waters, it is necessary to test model performance. Essentially, state-of-the-art climate simulations reflect the part of variability due to long-term signals, but do not account for interannual/decadal variability. Thus, it is more relevant to evaluate the skill of climate models to simulate trends. Unfortunately, the downscaled outputs of historical simulations offered by SimCLIM cover a short time span starting from 1995. With readily available data, it is found that the observed trend for 1995–2010 falls within the models' range, approaching the upper bound exactly (figure not shown), which demonstrates their ability to capture present climate tendency during the given period. Despite uncertainties in simulations, models are unanimous in their prediction of substantial SLR at Macau under greenhouse gas (GHG) increases, as we will see below.

As clarified in section 3.1, regional sea level change contains three contributions: GMSL change, departures from GMSL, and VLM. First, the future projected GMSL relative to 1986–2005 under four emissions scenarios is shown in Fig. 7. For each scenario, low, medium and high climate sensitiv-

ity projections are provided. Generally, climate sensitivity refers to the equilibrium change in surface air temperature following a unit change in radiative forcing. Since different GCMs produce different results for the same GHG emission scenarios, GCMs have different climate sensitivities. The GMSL is expected to rise for all emissions scenarios and climate sensitivities. Furthermore, the highest SLR is projected under the RCP8.5 scenario, and the lowest under the RCP2.6 scenario, which corresponds to the highest and lowest global warming in the future. In particular, the ranges of global SLR in 2100 are 28–61 cm, 36–71 cm, 38–73 cm and 53–98 cm under RCP2.6, RCP4.5, RCP6.0, and RCP8.5, respectively. If we combine emissions uncertainty and climate sensitivity uncertainty, the plausible GMSL change by 2100 ranges from 28 to 98 cm. Table 3 reports details of the GMSL changes, including the central estimate and likely range, for 2020, 2060, and 2100. At the beginning of this century, the magnitude of change in GMSL among different emission scenarios is fundamentally identical, indicating the limited effect of GHG concentration on the response of GMSL. However, the discrepancies in GMSL rise among different RCP scenarios become more and more noticeable as time progresses, especially at the end of the 21st century. Finally, it is noteworthy that the results yielded here are quite consistent with IPCC AR5 (Church et al., 2013).

Second, the regional departure from the GMSL in the scenario period is subsequently examined. The projected scaling factors in Macau for all climate models and their average are given in Fig. 8. There is a clear consensus among models (probability >85%) that sea level in Macau is likely to rise more rapidly than the global average, with the maximum scaling factor of 1.76 being recorded by CNRM-CM5. The scaling factors from HadGEM2-CC, HadGEM2-ES, and MIROC5, although less than 1, are very close to 1. Based on the multimodel ensemble mean, the ratio of local sea level change to the global average is 1.23, suggesting that the rate of SLR in Macau is 20% higher than the GMSL. In addition, as indicated by Fig. 9, faster SLR than the ocean as a whole occupies not only just Macau but indeed all over the coastal areas along SC, with a high degree of inter-model consistency. But what are the driving forces behind the greater-than-average SLR in Macau?

Table 3. Central estimate and range of GMSL change (cm) relative to 1986–2005 climatology under four emissions scenarios (RCP2.6, RCP4.5, RCP6.0, and RCP8.5). Results are presented for each emissions scenario. Values are the central estimate with the range in parentheses. The projected changes in the case of medium, low and high climate sensitivities are adopted as the central estimate, lower and upper bounds of the range.

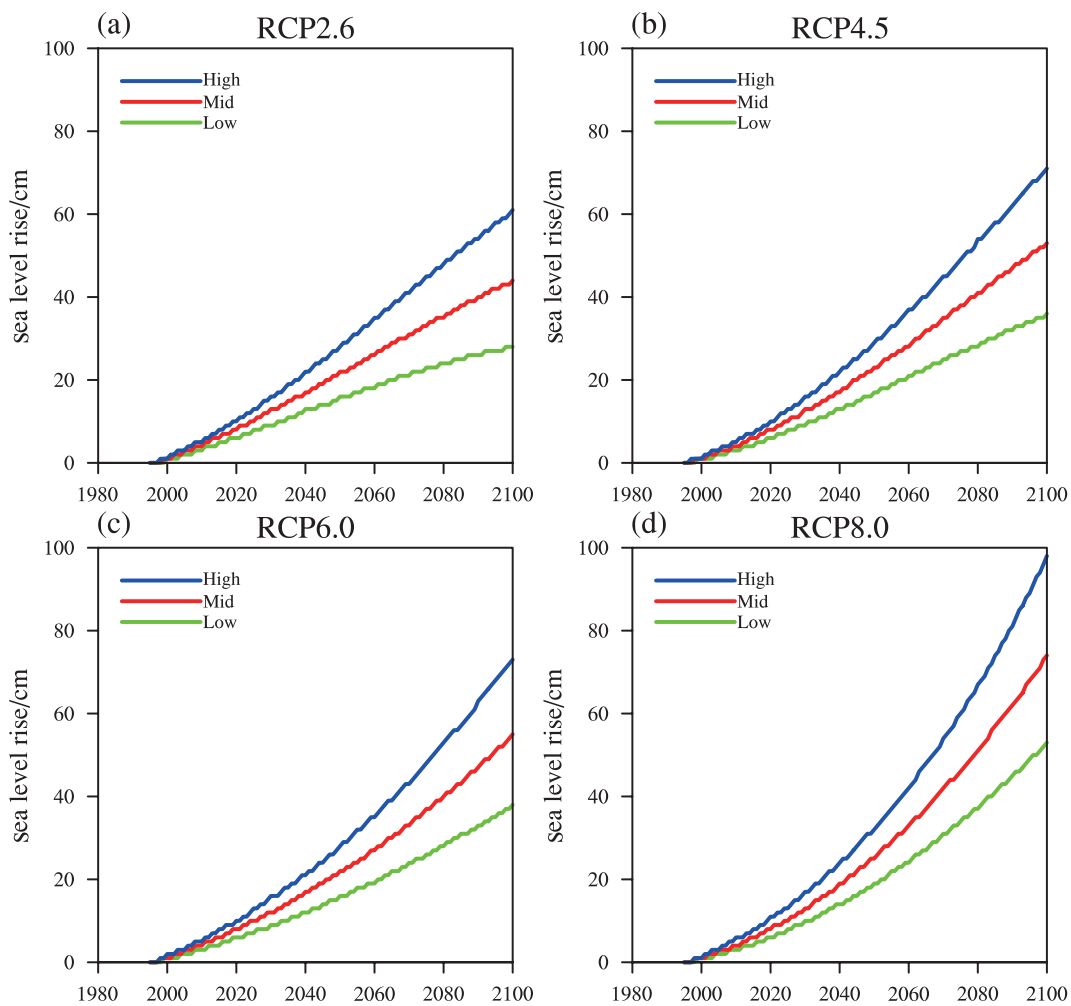|	2020	2060	2100
RCP2.6	8 (6–10)	26 (18–35)	44 (28–61)
RCP4.5	8 (6–10)	28 (21–37)	53 (36–71)
RCP6.0	8 (6–10)	27 (19–35)	55 (38–73)
RCP8.5	8 (6–11)	33 (24–42)	74 (53–98)

Fig. 7. Future projected changes in GMSL relative to 1986–2005 for low (green), medium (red) and high (blue) climate sensitivity under (a) RCP2.6, (b) RCP4.5, (c) RCP6.0 and (d) RCP8.5.
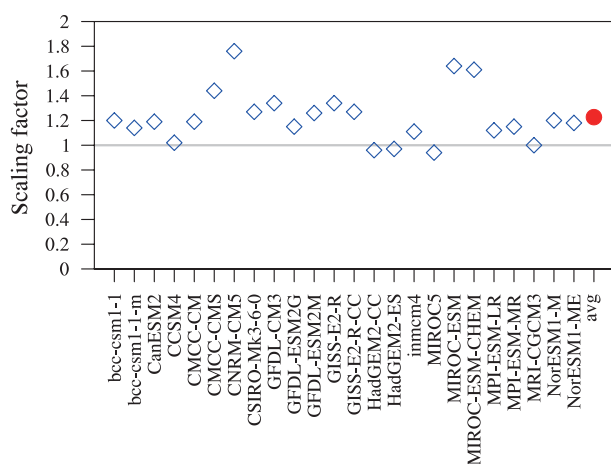

Fig. 8. Scaling factor in Macau for each model (blue diamonds) and the multimodel ensemble mean (red dot).

To address this problem, regional thermal conditions and dynamic processes that influence regional sea level are illumi-

nated. In terms of local thermal conditions, Fig. 10 shows the departures of local full depth OHC changes from the global average. The ocean along China's coastline appears to be warming more quickly than the global average, indicating an enhanced thermal expansion effect and thus higher sea level. In particular, the area adjacent to Macau is characterized by much stronger inter-model agreement, which persists throughout the 21st century. The inhomogeneous spatial pattern of projected oceanic heat gain is primarily a response to changes in air–sea fluxes and ocean circulation (Palmer, 2014). The downward net surface heat flux—the sum of shortwave radiation, longwave radiation, sensible heat flux and latent heat flux—around Macau and its adjacent seawaters exhibits an evident positive trend, indicating increased heat penetrating into the ocean (figure not shown). Apart from the influence of non-uniform increases in OHC, changes in regional atmospheric circulation also play an important role in generating an *in situ* sea level response through physical forcing of the wind. Based on the projected meridional wind signatures shown in Fig. 11, intensified southerlies with high inter-model coherence prevail over South China and the
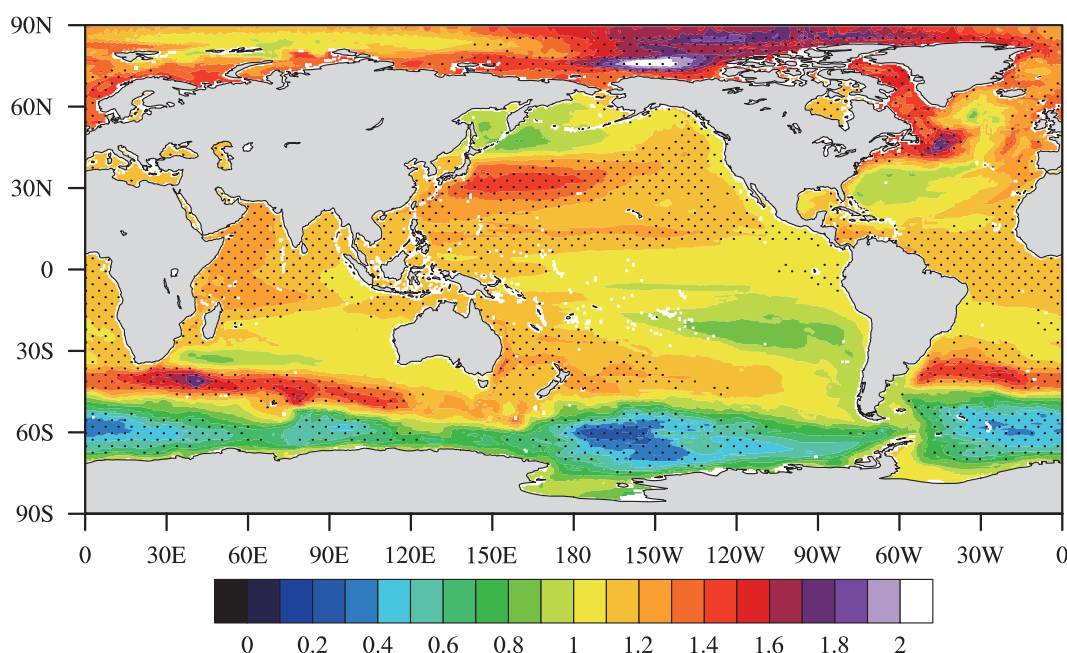
Fig. 9. Multimodel median for the projected scaling factor. Values greater than 1 indicate faster local sea level rise than global, and vice versa. Stippling indicates where at least 80% of all participating climate models have a scaling factor greater than 1 or less than 1.

surrounding region, which causes future SLR in Macau to be higher than the global average via the piling up of local water. But why does southerly wind tend to strengthen in future? With global warming, the temperature increase over land will be more rapid than that over the oceans, and the continental-scale land–sea thermal contrast will become larger in summer and smaller in winter. Therefore, it follows that the summer monsoon will be stronger and the winter monsoon weaker in the future, promoting intensified southerly anomalies (Sun and Ding, 2010). In short, faster SLR in Macau is connected with a stronger thermal expansion of local sea water and strengthened southerlies in the future.

The last component essential to creating a RSL rise scenario is the VLM-related trends. In Macau, however, the VLM makes little contribution to RSL change. Figures 12 and 13 illuminate the projected change in ASL and RSL (ASL combined with VLM), respectively. There is obvious high agreement between ASL and RSL, so in the following investigation we focus mainly on RSL (Fig. 13), which is the ultimate objective in this study. Despite the sea level in Macau tracking close to the global average (Fig. 7) throughout the entire 21st century, its amplitude is stronger. If we consider the worst-case RCP8.5 together with high climate sensitivity, for instance, sea level in Macau will rise by 118 cm, 20 cm above the global mean. The values associated with the projected SLR in Macau are shown in Table 4. Based on Fig. 13 and Table 4, three basic characteristics can be identified: (1) The higher emissions scenario leads to a more remarkable SLR than the lower emissions scenario: 90 cm under RCP8.5 versus 54 cm under RCP2.6 by 2100, for example, as a consequence of stronger ocean thermal expansion

Table 4. As in Table 3 but for Macau (units: cm).

	2020	2060	2100
RCP2.6	10 (8–12)	32 (22–43)	54 (35–74)
RCP4.5	10 (8–12)	34 (26–45)	65 (44–86)
RCP6.0	10 (8–12)	33 (24–43)	67 (47–88)
RCP8.5	10 (8–13)	40 (30–51)	90 (65–118)

and loss of mass from glaciers and ice sheets due to more rapid warming. Moreover, under RCP8.5 the linear trends for the periods 2020–2060 and 2060–2100 are 0.75 mm yr^{-1} and 1.25 mm yr^{-1}, respectively, highlighting the accelerating SLR in the future, which is also the case for RCP6.0. However, under RCP2.6 and RCP4.5, the SLR will remain at a moderate and steady rate. (2) The different emissions scenarios do not lead to dramatically different sea level responses during the beginning of the 21st century, but thereafter the projections begin to diverge. As shown in Table 4, all emissions scenarios predict a SLR of 10 cm, with a probable range from 8 cm to 12 cm, by 2020; however, by 2100 the projected sea levels under RCP8.5 reach 65–118 cm, double those under RCP2.6. (3) The climate sensitivity–related uncertainty tends to broaden with time, since the full ranges for 2020, 2060 and 2100 under RCP4.5 are 4 cm, 19 cm and 42 cm, respectively. In contrast, given the same climate sensitivity, the random uncertainty bounds are rather narrow, as indicated by the shading in Fig. 13. Consequently, the majority of the uncertainty originates from poor knowledge of climate sensitivity along with emissions levels, whereas other factors are likely to be secondary.
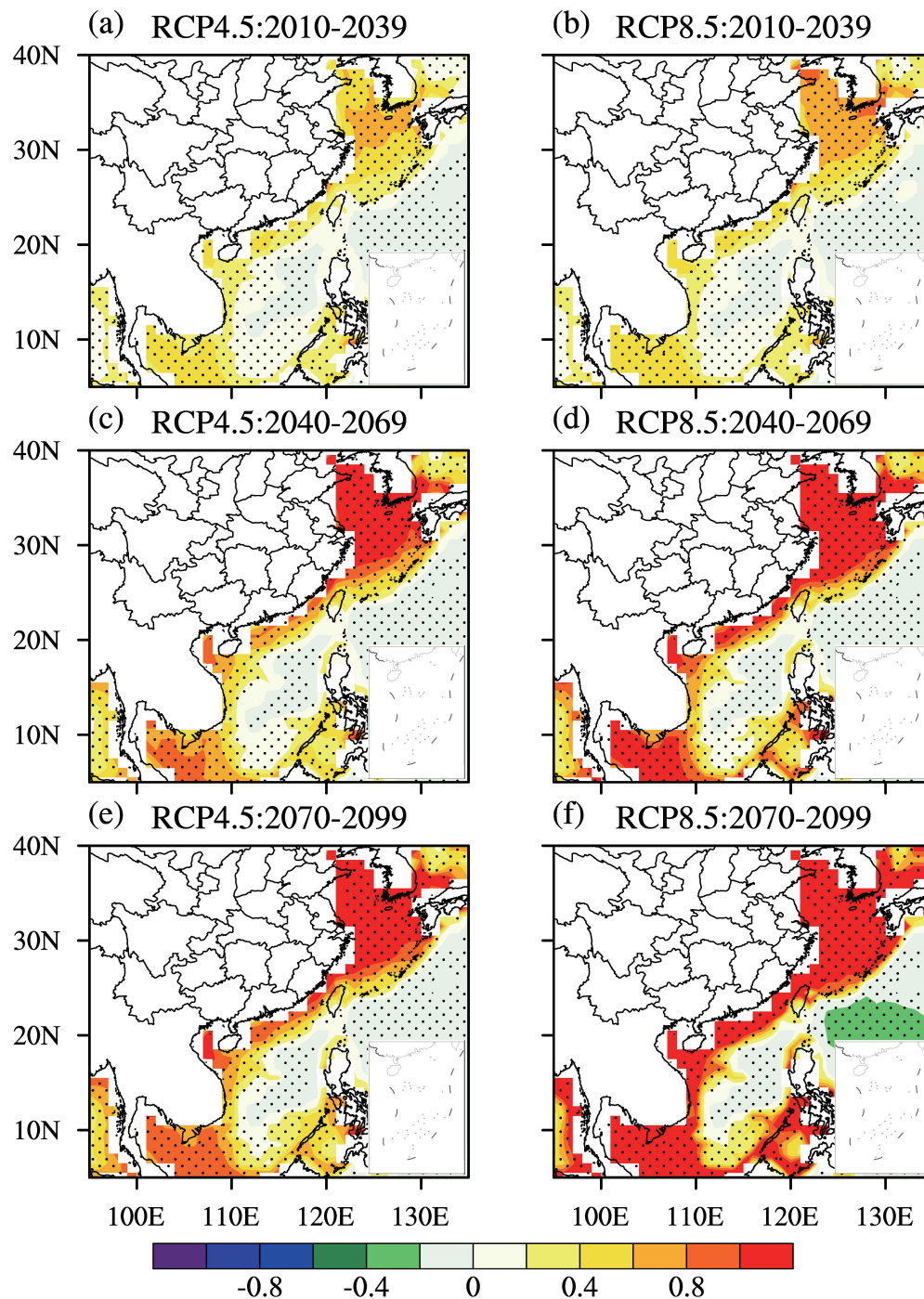
Fig. 10. Spatial pattern of the departure of local OHC change from the global average (units: °C) for (a, b) 2010–2039, (c, d) 2040–2069 and (e, f) 2070–2099 under (a, c, e) RCP4.5 and (b, d, f) RCP8.5. Stippling indicates where at least 75% of all GCMs agree on the sign. The red end of the color scale implies a faster rate of OHC increase compared to the global average, while the blue end denotes the opposite.

In short, the SLR in Macau by 2100 will span between a minimum of 35 cm and a maximum of 118 cm, depending on the emissions scenario and climate sensitivity. In addition, CMIP5 simulations give analogous patterns and magnitudes of future SLR along the entire coastline of SC compared to the changes in Macau, but are not detailed here.

6. Conclusions

Global warming-related SLR constitutes a substantial threat to Macau, due to its low elevation, small size and on-going land reclamation. This study was devised to determine the long-term variation of sea level change in Macau, as well as to develop future scenarios based on tide gauge and satel-
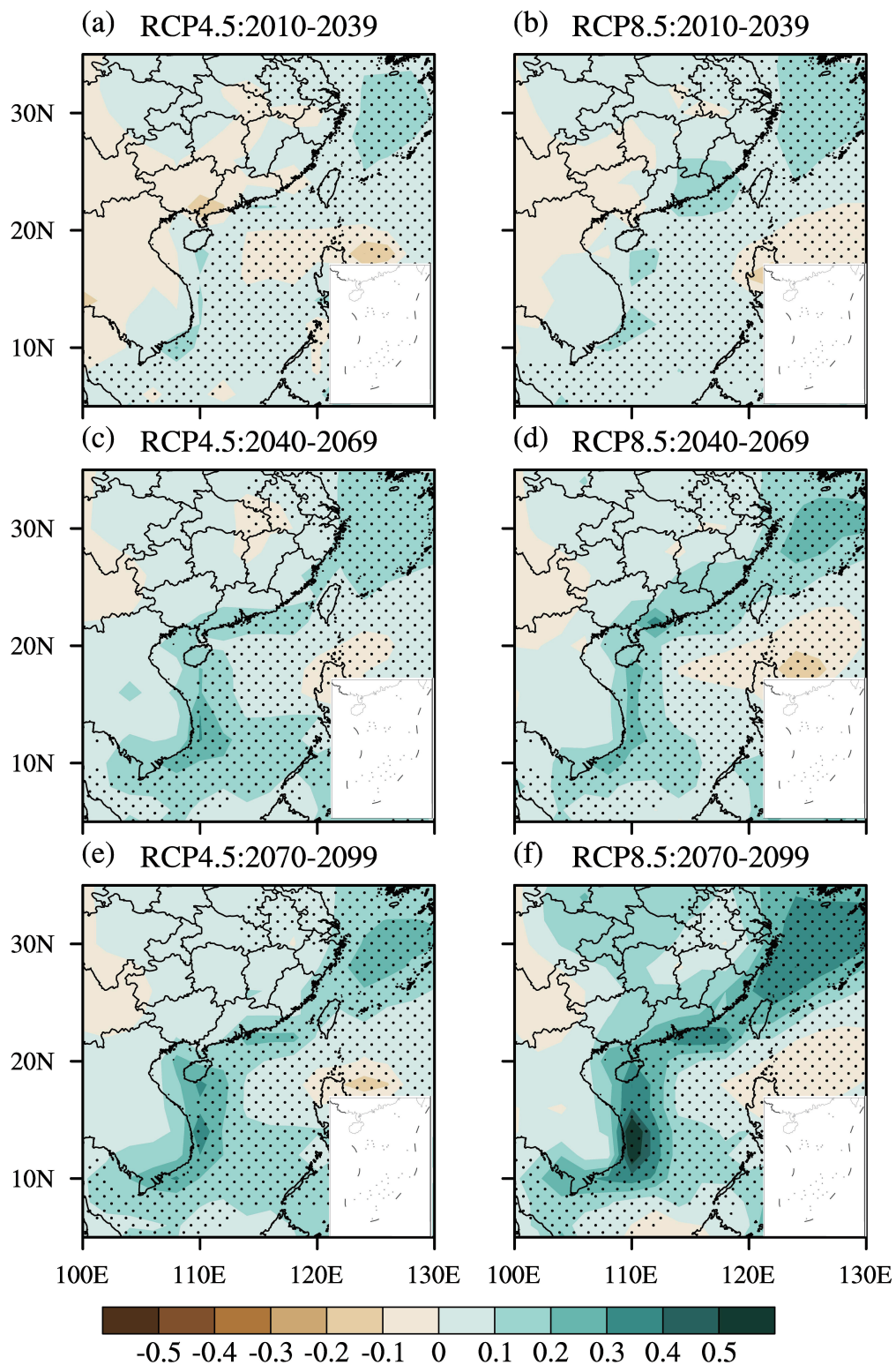
Fig. 11. Spatial pattern of meridional wind change at 1000 hPa (units: m s^{-1}) from the reference period (1986–2005) to (a, b) 2010–2039, (c, d) 2040–2069 and (e, f) 2070–2099 under (a, c, e) RCP4.5 and (b, d, f) RCP8.5. Stippling indicates where at least 75% of all GCMs agree on the sign. The cyan end of the color scale indicates southerly anomalies, while the brown end indicates the opposite.

lite data and GCM simulations, aiming to provide knowledge for SLR mitigation and adaptation.

Based on local tide gauge records, the rate of SLR shifted from about 1.35 mm yr^{-1} over 1925–2010 to 4.2 mm yr^{-1} over 1970–2010, reflecting an apparent acceleration of SLR. Despite the overall upward trend, the sea level in Macau also exhibits decadal variability. Furthermore, satellite altimetry data reveal that the sea level near Macau rose 10% faster than
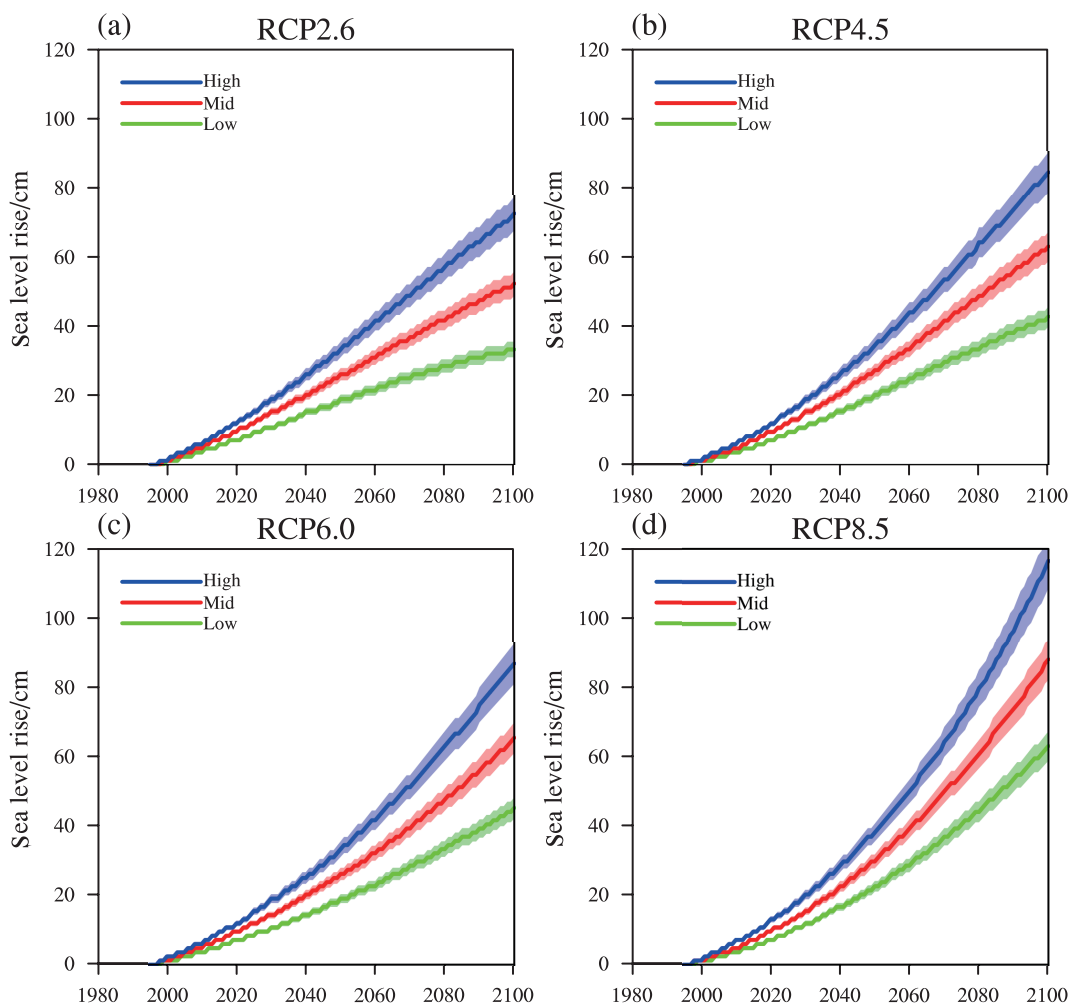
Fig. 12. As in Fig. 7 but for absolute SLR at Macau. Shading denotes the interquartile range across all climate models.

the global mean during the period from 1993 to 2012. Since the local sea level could be significantly adjusted by the rate of VLM, we subsequently derived it by calculating the linear trend of sea level difference between satellite altimetry and tide gauge measurements. The result indicates almost no rising or sinking of the landmass in Macau. However, complementary measurements based on high-accuracy GPS equipment co-located with the tide gauge at Macau should be implemented in the future to better monitor the rate of VLM.

As projected by a suite of climate models, the Macau SLR deviates positively from the global average by about 20%, indicating a 1.2 m SLR in Macau, corresponding to a unit increase of global average SLR. This is induced primarily by a greater-than-average rate of oceanic thermal expansion in Macau, together with enhanced southerly anomalies that lead to a piling up of sea water. Specifically, RSLs with the local rate of VLM added indicate a rise of 8–12, 22–51, and 35–118 cm by 2020, 2060 and 2100 with respect to the 1986–2005 baseline climatology, respectively, with the amount of rise dependent on the emissions scenario and climate sensitivity. If we consider the medium emissions scenario RCP4.5 along with medium climate sensitivity, Macau can expect to experience an SLR of 10, 34 and 65 cm by

2020, 2060 and 2100. If the worst case happens (RCP8.5 plus high climate sensitivity), the SLR will be far higher than that in the medium case; namely, 13, 51 and 118 cm by 2020, 2060, and 2100, respectively. The SLR under the lower emissions scenario is expected to be less severe than that under the higher emissions scenarios: by 2100, an SLR of 65–118 cm in Macau under RCP8.5, almost twice as fast as that under RCP2.6. Moreover, the SLR will accelerate under RCP6.0 and RCP8.5, while remaining at a moderate and steady rate under RCP4.5 and RCP2.6. The GHG forcing scenario has virtually no influence on the projected change during the beginning of this century, but its impact on divergent sea level responses becomes noticeable after the middle of the century. The majority of the projection uncertainty comes from the emissions scenario and poor knowledge of climate sensitivity. By 2020, the uncertainty range is only 4 cm, yet by 2100 the range will be increased to 83 cm. Moreover, the sea level changes in the past and future over the whole of SC to a large extent resemble that in Macau.

This study concerns scenario development, which is only the first step in the whole process. Additional problems need to be addressed, as follows: (1) Given the large uncertainties in future projections, the obvious question is how to select
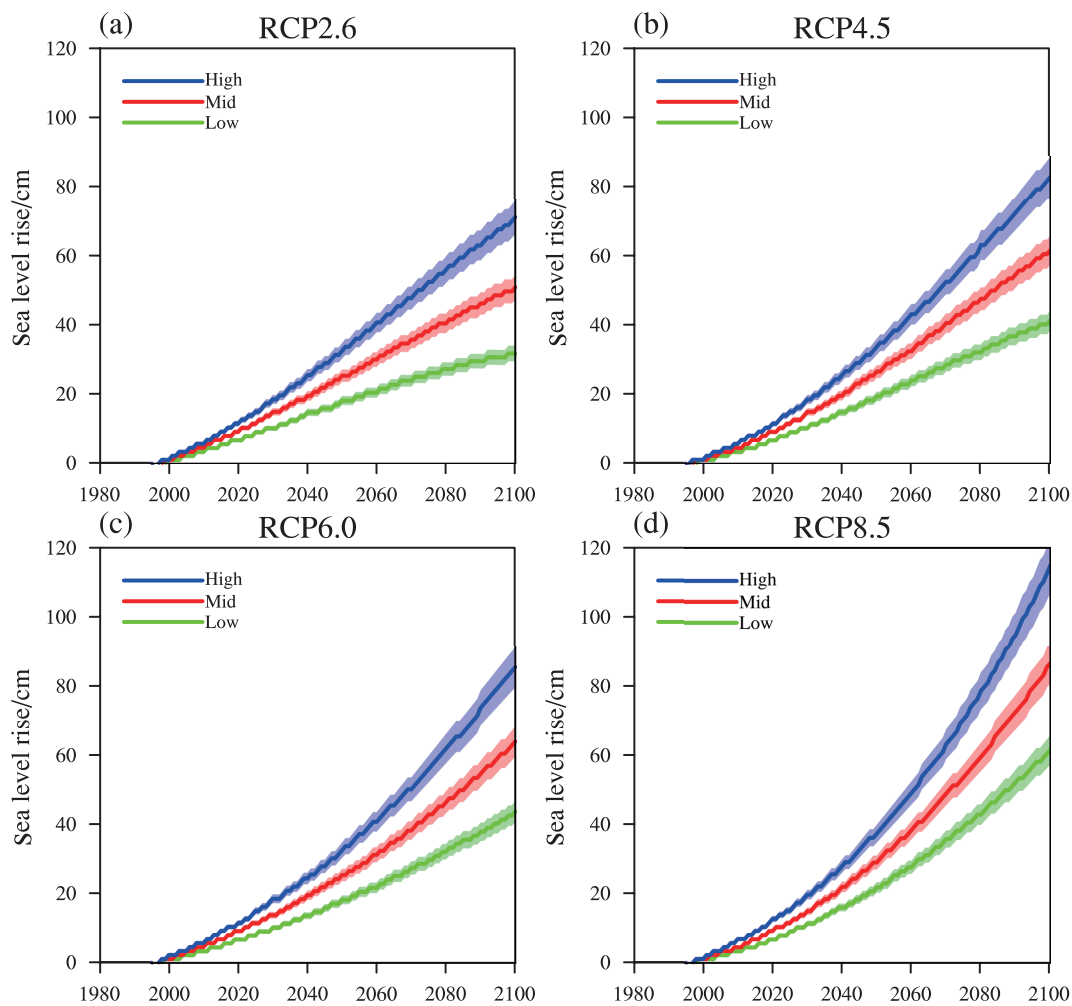
Fig. 13. As in Fig. 12 but for relative SLR (incorporating VLM) at Macau.

appropriate SLR values. Consequently, continuous monitoring of actual SLR, and understanding of which emissions scenario and climate sensitivity is the most realistic, are essential to the scenario choice. (2) Extreme high-water events (short-term phenomena) in Macau are not examined in this study, but they must be recognized in impact analysis. Although rising sea level will increase the probability of storm surges and waves, quantitative assessments of such risks are inevitable in the future. (3) And last but not least, what are the most suitable adaptation policies and planning objectives in Macau? In general, we need to combine the consequences of SLR and the potential costs incurred in future adaptations. Therefore, feasible mitigation and adaptation strategies should be initiated to address SLR.

REFERENCES

BakiIz, H., and C. K. Shum, 2000: Mean sea level variation in the South China Sea from four decades of tidal records in Hong Kong. *Marine Geodesy*, **23**, 221–233.

Cazenave, A., K. Dominh, F. Ponchaut, L. Soudarin, J. F. Cretaux, and C. Le Provost, 1999: Sea level changes from Topex-Poseidon altimetry and tide gauges, and vertical crustal motions from DORIS. *Geophys. Res. Lett.*, **26**, 2077–2080.

Chen, D. L., and A. Omstedt, 2005: Climate-induced variability of sea level in Stockholm: Influence of air temperature and atmospheric circulation. *Adv. Atmos. Sci.*, **22**, 655–664, doi: 10.1007/BF02918709.

Church, J. A., and N. J. White, 2006: A 20th century acceleration in global sea-level rise. *Geophys. Res. Lett.*, **33**, L01602, doi: 10.1029/2005GL024826.

Church, J. A., and N. J. White, 2011: Sea-level rise from the late 19th to the early 21st century. *Surveys in Geophysics*, **32**, 585–602.

Church, J. A., and Coauthors, 2013: Sea Level Change. *Climate Change 2013: The Physical Science Basis. Contribution of Working Group I to the Fifth Assessment Report of the Intergovernmental Panel on Climate Change*, T. F. Stocker, et al., Eds., Cambridge University Press, Cambridge, United Kingdom and New York, NY, USA, 1137–1216.

Dibarboure, G., O. Lauret, F. Mertz, V. Rosmorduc, and C. Maheu, 2014: SSALTO/DUACS user handbook: (M) SLA and (M) ADT near-real time and delayed time products. Rep. CLS-DOS-NT-06-034, 69 pp.

Ding, X., D. Zheng, Y. Chen, J. Chao, and Z. Li, 2001: Sea level change in Hong Kong from tide gauge measurements of 1954–1999. *Journal of Geodesy*, **74**, 683–689.

García, D., I. Vigo, B. F. Chao, and M. C. Martínez, 2007: Vertical crustal motion along the Mediterranean and Black Sea coast derived from ocean altimetry and tide gauge data. *Pure Appl. Geophys.*, **164**, 851–863.

He, L., G. S. Li, K. Li, and Y. Q. Shu, 2014: Estimation of regional sea level change in the Pearl River Delta from tide gauge and satellite altimetry data. *Estuarine, Coastal and Shelf Science*, **141**, 69–77.

Li, K., and H. Mok, 2011: Long term trends of the regional sea level changes in Hong Kong and the adjacent waters. *The 6th International Conference on Asian and Pacific Coasts (APAC2011)*, Hong Kong, HKO Reprint No. 990.

Mitchell, T. D., 2003: Pattern scaling: An examination of the accuracy of the technique for describing future climates. *Climatic Change*, **60**, 217–242.

Moron, V., and A. Ullmann, 2005: Relationship between sea-level pressure and sea-level height in the Camargue (French Mediterranean coast). *Inter. J. Climatol.*, **25**, 1531–1540.

Moss, R. H., and Coauthors, 2010: The next generation of scenarios for climate change research and assessment. *Nature*, **463**, 747–756.

Nerem, R. S., D. P. Chambers, C. Choe, and G. T. Mitchum, 2010: Estimating mean sea level change from the TOPEX and Jason altimeter missions. *Marine Geodesy*, **33**, 435–446.

Nicholls, R. J., and A. Cazenave, 2010: Sea-level rise and its impact on coastal zones. *Science*, **328**, 1517–1520.

Nicholls, R., S. E. Hanson, J. A. Lowe, R. A. Warrick, X. Lu, A. J. Long, and T. R. Carter, 2011: Constructing sea-level scenarios for impact and adaptation assessment of coastal areas: A guidance document. *Supporting Material, Intergovernmental Panel on Climate Change Task Group on Data and Scenario Support for Impact and Climate Analysis* (*TGICA*), Geneva, Switzerland, 47 pp.

Palmer, M. D., 2014: Variations of Oceanic Heat Content. *Global Environmental Change*, Freedman, B., Ed., Springer Netherlands, 77–83.

Ray, R. D., B. D. Beckley, and F. G. Lemoine, 2010: Vertical crustal motion derived from satellite altimetry and tide gauges, and comparisons with DORIS measurements. *Advances in Space Research*, **45**, 1510–1522.

Santer, B. D., T. M. L. Wigley, M. E. Schlesinger, and J. F. B. Mitchell, 1990: Developing climate scenarios from equilibrium GCM results. MPI for Meteorology, Report No. 47, Hamburg, 29 pp.

Stephens, S. A., and R. G. Bell, 2009: Review of Nelson City minimum ground level requirements in relation to coastal inundation and sea-level rise. HAM2009-124, National Institute of Water and Atmospheric Research Ltd. 58 pp.

Sun, Y., and Y. H. Ding, 2010: A projection of future changes in summer precipitation and monsoon in East Asia. *Science China Earth Sciences*, **53**, 284–300.

Taylor, K. E., R. J. Stouffer, and G. A. Meehl, 2012: An overview of CMIP5 and the experiment design. *Bull. Amer. Meteor. Soc.*, **93**, 485–498.

Walsh, K. J. E., D. R. Jackett, T. J. McDougall, and A. B. Pittock, 1998: Global warming and sea-level rise on the Gold Coast. Report Prepared for the Gold Coast City Council, Mordialloc, Australia, CSIRO Atmospheric Research, 34 pp.

Warrick, R. A., W. Ye, P. Kouwenhoven, J. E. Hay, and C. Cheatham, 2005: New developments of the SimCLIM model for simulating adaptation to risks arising from climate variability and change. *Proceedings of the International Congress on Modelling and Simulation, Modelling and Simulation Society of Australia and New Zealand*, Zerger, A., and R. M. ARGENT, Eds. Canberra, Australia, 170–176.

Wong, W. T., K. W. Li, and K. H. Yeung, 2003: Long term sea level change in Hong Kong. *Hong Kong Meteorological Society Bulletin*, **13**, 24–40.